Pion-Pion Interactions in the States $T=0$ and $T=1$*

T. D. SPEARMAN†
Department of Physics, University College, Gower Street, London, England
(Received 17 September 1962)

New dispersion relations are derived for the s-wave pion-nucleon scattering amplitudes. These relations are specifically chosen to facilitate the task of separating the two-pion exchange term from the other effects contributing to low-energy pion-nucleon scattering. In these equations the contribution from the unknown short-range terms is markedly suppressed, a greater emphasis is placed on the experimentally better established very low energy pion-nucleon data, in particular on the scattering lengths, and in the contribution of the two-pion exchange term the lower energies are more heavily stressed. The terms due to the two-pion exchange, which we isolate, are very clearly recognized by their characteristic energy dependences.

The two-pion exchange terms are analyzed in terms of the interaction between the two pions. The values obtained for these terms are made to yield information about the phase shifts for pion-pion scattering in the $T=1$ and $T=0$ states.

In the $T=1$ state the data are well fitted with a narrow p-wave resonance in the pion-pion system at 750 MeV. Taking the results of electron-nucleon scattering experiments in conjunction with the present data, the half-width of this resonance is found to lie between 40 and 60 MeV, in agreement with the experimental data for the observed ρ meson.

In the $T=0$ state the data are fitted with a two-parameter form for the s-wave pion-pion phase shift. Both of these parameters are not simultaneously determined by the present data. As an added restriction on the phase shift it is required to lead to agreement with the experimental results for the process $p+d \rightarrow \mathrm{He}^3+2\pi$. This singles out a $T=0$ s-wave phase shift with a scattering length of $a_0 \approx 1.6$ (units $\hbar=\mu=c=1$).

1. INTRODUCTION

THE concept of a nucleon possessing "structure" is a well-established one, both experimentally and theoretically.[1] This structure is envisaged phenomenologically as a "cloud" of virtual strongly interacting particles surrounding a central core. The outermost particles of this "cloud" will be the lightest ones, the pions. When pions are scattered by nucleons, a part of their interaction will be with these virtual pions of the "cloud." If a suitable method of analysis were available, it should thus be possible to derive information about pion-pion interactions from the experimental data on pion-nucleon scattering.

In the language of dispersion relations the interaction between the scattered pions and the pions of the nucleon cloud is represented as the two-pion or many-pion exchange terms. A method has recently been developed[2-4] to isolate the two-pion exchange term from the other terms contributing to pion-nucleon scattering. This method involves partial-wave dispersion relations for pion-nucleon scattering and uses the s-wave pion-nucleon phase shifts to determine the two-pion exchange term. The two-pion exchange term can be analyzed in terms of the interactions between the two pions and information has thus been obtained about pion-pion scattering in the $T=0$ and $T=1$ states.[5]

In the present paper, a refined form of the above method for analyzing pion-nucleon scattering is presented and applied. This uses new dispersion relations which are specifically chosen so that the two-pion exchange term may be isolated in a more decisive and clear-cut way.

The results obtained for the two-pion exchange term are analyzed to give information about the $T=1$ and $T=0$ pion-pion phase shifts. The $T=1$ data are found to be well explained by a p-wave pion-pion resonance at 750 MeV corresponding to the experimentally observed ρ meson.[6] Because of the high energy of the ρ meson, the approximations normally made in solving the integral equations for the amplitudes $\pi+\pi \rightarrow N+\bar{N}$ break down. Without information about four-pion states it seems that we cannot solve the equation and thus determine the $T=1$, $J=1$ pion-pion phase shift. We can instead, however, combine the results of electron-nucleon scattering experiments with the present data and this enables us to predict a value for the width of the ρ meson which is in agreement with the experimentally observed values.

To fit the $T=0$ data we use a two-parameter form for the s-wave pion-pion phase shift. Fitting with the present data only determines one of these parameters. To fix the second parameter we use the experimental data obtained by Abashian, Booth, and Crowe[7] for the

* This work has been supported in part by the Air Office of Scientific Research OAR (European Office, Aerospace Research USAF).

† Present address: Department of Physics, University of Illinois, Urbana, Illinois.

[1] See, for example, S. D. Drell and F. Zachariasen, *Electromagnetic Structure of Nucleons* (Oxford University Press, New York, 1961).

[2] J. Hamilton, P. Menotti, and T. D. Spearman, Ann. Phys. (N. Y.) **12**, 172 (1961). We refer to this paper as I.

[3] J. Hamilton, P. Menotti, T. D. Spearman, and W. S. Woolcock, Nuovo Cimento **20**, 519 (1961). We refer to this paper as II.

[4] J. Hamilton, T. D. Spearman, and W. S. Woolcock, Ann. Phys. (N. Y.) **17**, 1 (1962). We refer to this paper as III.

[5] J. Hamilton, P. Menotti, G. C. Oades, and L. L. J. Vick (to be published). We refer to this paper as IV.

[6] For a comprehensive bibliography see M. L. Stevenson, University of California Lawrence Radiation Laboratory Report, UCRL-9999 (unpublished).

[7] A. Abashian, N. E. Booth, and K. M. Crowe, Phys. Rev. Letters **7**, 35 (1961).

process $p+d\rightarrow \mathrm{He}^3+2\pi$. If we impose the requirement on the $T=0$, $J=0$ phase shift that, as well as satisfying the requirements from pion-nucleon scattering, it also leads to agreement with the above experimental data, we find that this phase shift is now uniquely determined. Good agreement with the above experimental data is obtained.

In Sec. 2 we introduce the necessary notation and describe the new dispersion relations. In Sec. 3 we present the calculated values for the two-pion exchange terms and discuss their analysis. In Sec. 4 we discuss the process $p+d\rightarrow \mathrm{He}^3+2\pi$ and fit the experimental data with a two-pion final-state interaction. In Sec. 5 we conclude and summarize the results.

2. THE NEW DISPERSION RELATIONS

A. Notation

We shall summarize the notation, which is the same as in I.

The invariant scalar amplitudes $A^{\pm}(s,t,\bar{s})$, $B^{\pm}(s,t,\bar{s})$ are related to the amplitudes with isotopic spin $T=\frac{3}{2}$, $T=\frac{1}{2}$ (in the pion-nucleon channel) as follows:

$$A^{+}=\tfrac{1}{3}(A^{1/2}+2A^{3/2}),$$
$$A^{-}=\tfrac{1}{3}(A^{1/2}-A^{3/2}), \tag{1}$$

and similarly for $B^{\pm}$. We shall refer to the pion-nucleon scattering channel as channel 3, the crossed pion-nucleon channel as channel 1, and the channel $\pi+\pi\rightarrow N+\bar{N}$ as channel 2. The squares of the energy in the center-of-mass system in these three channels are s, $\bar{s}$, and t, respectively. The amplitudes A^{+}, B^{+} refer to isotopic spin $T=0$ and A^{-}, B^{-} to $T=1$ in channel 2.

To relate the partial-wave amplitudes to the invariant amplitudes we define functions

$$f_1^{(T)}=\frac{(W+M)^2-1}{16\pi W^2}[A^{(T)}+(W-M)B^{(T)}],$$
$$f_2^{(T)}=\frac{(W-M)^2-1}{16\pi W^2}[-A^{(T)}+(W+M)B^{(T)}], \tag{2}$$

where $W=\sqrt{s}$, M is the nucleon mass, and we have put the pion mass equal to unity. The superscripts T denote the isotopic spin of the pion-nucleon system in channel 3. The s-wave pion-nucleon amplitudes $f_0^T(s)$ are given in terms of $f_1^{(T)}$, $f_2^{(T)}$ by

$$f_0^T(s)=\tfrac{1}{2}\int_{-1}^{1}dx\,(f_1^{(T)}+xf_2^{(T)}), \tag{3}$$

where $x=\cos\theta$, θ is the center-of-mass scattering angle for channel 3, and

$$f_0^T(s)\equiv e^{i\delta_T}\sin\delta_T/q$$

are the s-wave scattering amplitudes. q is the magnitude of the center-of-mass momentum in channel 3 and δ_T are the s-wave pion-nucleon phase shifts.

B. Analytic Properties

The Mandelstam representation tells us the singularities of the invariant amplitudes $A^{\pm}(s,t,\bar{s})$, $B^{\pm}(s,t,\bar{s})$. We may use Eqs. (2) and (3) to deduce the singularities of $f_0^T(s)$. These singularities are shown in Fig. 1. A detailed discussion of these singularities has been given by Kennedy and the present author.[8] Knowing these singularities we could proceed as in I–IV to write dispersion relations for $f_0^T(s)$. We shall instead define a new function

$$g_0^T(s)=f_0^T(s)/B(s), \tag{4}$$

where

$$B(s)=\{[s-(M-1)^2][(M+1)^2-s]\}^{1/2}. \tag{5}$$

$B(s)$ is defined in the cut s plane with cuts along the real axis from $-\infty$ to $(M-1)^2$ and from $(M+1)^2$ to ∞ so as to be real and positive on the real axis between $(M-1)^2$ and $(M+1)^2$. We shall now consider the properties of $g_0^T(s)$.

It follows from the definition of $B(s)$ that, as shown in Fig. 2, when ϵ is a small positive quantity,

$$B(s+i\epsilon)=-i|B(s)|,$$
$$B(s-i\epsilon)=+i|B(s)|, \quad \text{for } s \text{ real} \geqslant (M+1)^2;$$

and

$$B(s+i\epsilon)=+i|B(s)|,$$
$$B(s-i\epsilon)=-i|B(s)|, \quad \text{for } s \text{ real} \leqslant (M-1)^2.$$

It follows from these relations that for real s:

$$g^T(s+i\epsilon)-g^T(s-i\epsilon)=\pm 2i[\mathrm{Re}f_0^T(s)/|B(s)|], \tag{6}$$

according as $s\gtrless(M+1)^2$ or $s\lessgtr(M-1)^2$.

When s lies on the circle $|s|=M^2-1$, we may show that, if $s=(M^2-1)e^{i\phi}$,

$$B(s)=e^{i\phi/2}|B(s)|. \tag{7}$$

This is seen from Fig. 2.

By definition

$$B(s)=(AC\times BC)^{1/2}e^{i(\phi_1-\phi_2)/2}.$$

Since $OA\times OB=OC^2$, it follows that the triangles

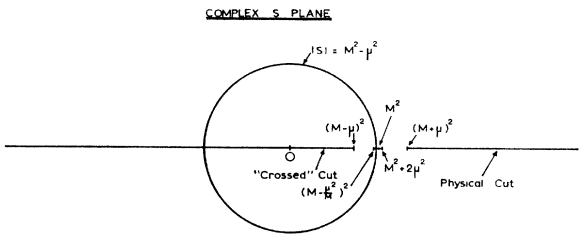

FIG. 1. Location of the singularities of the pion-nucleon partial-wave amplitudes in the complex s plane.

[8] J. Kennedy and T. D. Spearman, Phys. Rev. 126, 1596 (1962).

OAC, OCB are similar and so that $\phi_2=\angle OCA$. So

$$\phi_1-\phi_2=\phi.$$

The singularities of $g_0^T(s)$ in the s plane will be the same as those of $f_0^T(s)$, i.e., those shown in Fig. 1. The only singularities introduced by the factor $1/B(s)$ are the cuts on the real axis from $-\infty$ to $(M-1)^2$ and from $(M+1)^2$ to ∞ and these are already present in $f_0^T(s)$.

C. The Dispersion Relations

We may now write the following dispersion relations for $g_0^T(s)$:

$$\begin{aligned}\mathrm{Re}g_0^T(s)&=-\frac{1}{\pi}\int_{(M+1)^2}^{\infty}\frac{\mathrm{Re}f_0^T(s')}{|B(s')|(s'-s)}ds'\\&\quad-\frac{1}{\pi}\int_{(M-1)^2}^{M^2+2}\frac{\mathrm{Im}f_0^T(s')}{|B(s')|(s'-s)}ds'\\&\quad+\frac{1}{\pi}\int_{0}^{(M-1)^2}\frac{\mathrm{Re}f_0^T(s')}{|B(s')|(s'-s)}ds'\\&=-\frac{1}{\pi}\int_{-\infty}^{0}\frac{\mathrm{Re}f_0^T(s')}{|B(s')|(s'-s)}+\frac{R_0^T}{s}\\&\quad+\frac{1}{2\pi i}\int_{\text{circle}}\frac{\Delta f_0^T(s')e^{-i\phi'/2}}{|B(s')|(s'-s)}ds'\\&=\mathfrak{D}^T(s).\end{aligned}\tag{8}$$

A "principal value" is to be taken for any integral in which $(s'-s)^{-1}$ becomes singular. $\Delta f_0^T(s')$ is the discontinuity in $f_0^T(s')$ across the circle. R_0 is the residue of a possible pole at the origin. We have used Eqs. (6) and (7) to express the integrands in terms of $f_0^T(s)$. We follow the notation of I-IV and call $\mathfrak{D}^T(s)$ the "discrepancies." It is clear that

$$\mathrm{Re}g_0^T(s)=-\mathrm{Im}f_0^T(s)/B(s),\quad\text{for real } s\geqslant(M+1)^2,$$
$$\mathrm{Re}g_0^T(s)=+\mathrm{Im}f_0^T(s)/B(s),\quad\text{for real } s\leqslant(M-1)^2.$$

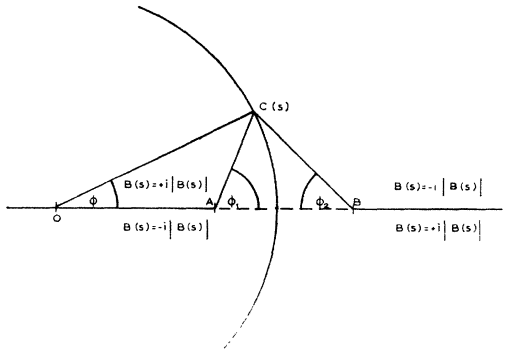

FIG. 2. Properties of the function $B(s)\equiv\{[s-(M-1)^2]\times[(M+1)^2-s]\}^{1/2}$ in the complex s plane.

All the terms on the left-hand side of Eq. (8) can be evaluated in terms of the low-energy pion-nucleon data[9] for values of s above $(M+1)^2=59.6$ up to, say, 76. These terms can also be evaluated, using the "crossing relations" for the amplitudes $A^{\pm}(s,t,\bar{s})$, $B^{\pm}(s,t,\bar{s})$, for s below $(M-1)^2=32.2$ down to, say, 20. The crossing procedure introduces all partial waves but for $s\gtrsim 20$ we shall not be concerned with very high energies in the crossed channel and it suffices to consider s, p, d waves. So we can evaluate $\mathfrak{D}^T(s)$ in the regions $20\leqslant s\leqslant 32.2$ and $59.6\leqslant s\leqslant 76$.

D. Separation of the Two-Pion Exchange Term

The term which we wish to isolate is the third on the right-hand side or rather the part of that term coming from the front of the circle, say $|\phi|\leqslant 60°$ where $s=(M^2-1)e^{i\phi}$. The circle cut comes from the denominators $t'-t$ which means that it arises from channel 2 processes, $\pi+\pi\rightarrow N+\bar{N}$. Low energies in this channel correspond to the two-pion exchange term in pion-nucleon scattering. Although a single value of t does not map onto a single point in the s plane on account of the x integration in Eq. (3), it maps into a range of points which has the property that as t increases above 4 the smallest phase angle ϕ on the circle increases. Thus for each value of ϕ we get a maximum value of t contributing. So the front of the circle, say $|\phi|\leqslant 60°$, is restricted to the lower energies in channel 2 and arises primarily from the two-pion exchange.

The way in which we separate out the contribution from the front of the circle to $\mathfrak{D}^T(s)$ is the same as that used in II, III, and IV. But in the present case the isolation of this term is made much more simple by the special properties of Eq. (8) which we shall discuss below when we compare this equation with the analogous one in I–IV.

To distinguish the term from the front of the circle from the other terms contributing to $\mathfrak{D}^T(s)$, we "attack this term on both flanks." We evaluate $\mathfrak{D}^T(s)$ both in the physical region $s\geqslant(M+1)^2$ and in the "crossed" region $s\leqslant(M-1)^2$. Since the front of the circle lies between these two regions, we might expect that the term arising from this should show a marked variation of energy dependence between these regions. That this is so is clearly seen from the results in Figs. 3 and 4. The energy dependence in both of these graphs, as shown by the solid lines, is in fact due entirely to the front of the circle: The contribution from the other terms is well represented by a constant. It is clear, however, that even if the remaining terms did contribute an energy-dependent effect, this could be separated from the very characteristic energy dependences associated with the front of the circle both in the case of $\mathfrak{D}^-(s)$ and $\mathfrak{D}^+(s)$.

Because of the proximity of the front of the circle

[9] The third term on the left of Eq. (8) involves only the pion-nucleon coupling constant f^2. It is evaluated using $f^2=0.081$.

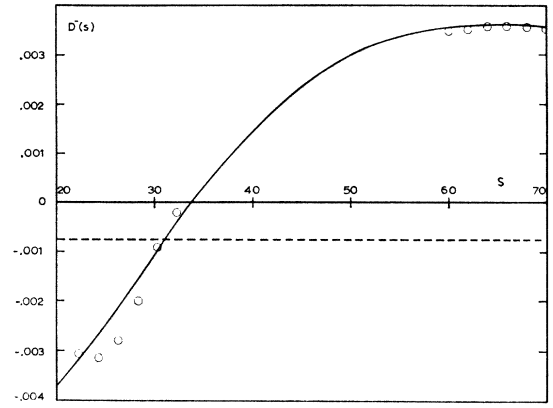

FIG. 3. $\mathfrak{D}^-(s)$. The calculated values are represented by small circles. The solid curve is $\mathfrak{D}_{\pi\pi}{}^-(s)$, for a δ function at $t=28$ with $C_1=-1.4$ and integration on the circle only for $|\phi|\leqslant 60°$, plus a short-range constant term represented by the dashed line.

to the physical region we interpret this as giving rise to a long-range interaction. We have seen above that as the phase angle ϕ on the circle increases, so does the maximum value of t introduced at that point. In other words, as we move on the circle further away from the physical region, the mass of the exchanged system is permitted to increase thus causing forces of shorter range. Similarly we interpret the remaining terms on the right of Eq. (8), coming from beyond the origin, as being associated with short-range forces. A discussion of this relation between the position of singularities and the range of the corresponding forces is given in III.

E. Comparison with the Earlier Method

Equation (8) differs from the corresponding equation used in I–IV in two important respects. The main consequences of these differences are (1) to suppress the terms other than from the front of the circle on the right of Eq. (8); (2) to emphasize more heavily the lower t values in the contribution from the front of the circle, and (3) on the left-hand side of Eq. (8) to lay more stress on the contribution from very low energy pion-nucleon data, which are best established experimentally, and in particular on the scattering lengths.

These two main points of difference are: Firstly, the integrals over the real axis singularities involve $\mathrm{Re}f_0{}^T(s)$ instead of $\mathrm{Im}f_0{}^T(s)$. This fact in itself leads to a suppression of the short-range, or high-energy, effects since at high energies interaction amplitudes are expected to become largely imaginary. Secondly, and of great importance for the present application, the integrands contain the weighting factor $|B(s')|^{-1}$. This factor is responsible for the desired effect of suppressing the short-range effects, of emphasizing the contribution of the low-energy pion-nucleon data, and of stressing the lower energies of the two-pion system in the exchange graph.

The suppression of the effect of distant singularities is clearly seen since for large $|s'|$, $|B(s')|^{-1}$ is like $1/s'$. On the other hand, when we come near to the thresholds $(M\pm1)^2$, we see that $|B(s')|^{-1}$ diverges as $|s-(M\pm1)^2|^{-1/2}$. This divergence disappears on integration but it clearly stresses heavily the values of $\mathrm{Re}f_0{}^T(s')$ at the two thresholds, which depend on the scattering lengths a_1, a_3. Representative values of $|B(s')|^{-1}$ along the real axis are shown in Table I. On the front of the circle $|B(s')|^{-1}$ decreases as we move away from the real axis, i.e., as $|\phi|$ increases. This causes the lower energies in the two-pion system to be stressed. Values of $|B(s')|^{-1}$ for different values of the phase angle ϕ' are shown in Table II.

On the front of the circle, and particularly for the smallest values of t which are most heavily stressed, $\phi/2$ is small. Consequently the factor $e^{-i\phi/2}$ in the third term on the right of Eq. (8) is approximately real. This means that the s dependence of this term should be approximately similar to that of the corresponding term in papers II, III, and IV. That this is so is seen from a comparison of Figs. 3 and 4 with the corresponding graphs in III.

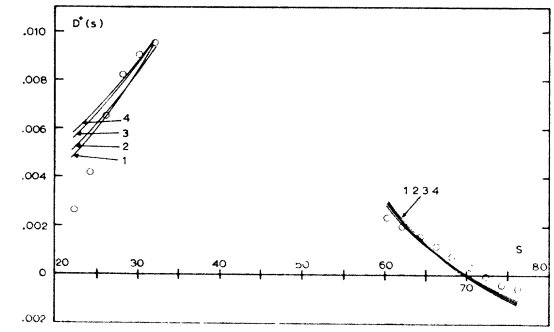

FIG. 4. $\mathfrak{D}^+(s)$. The calculated values are represented by small circles. The solid curves correspond to solutions 1 to 4 of Table III plus short-range constant terms lying between -0.0048 and -0.0051.

3. CALCULATION AND ANALYSIS OF THE TWO-PION EXCHANGE TERMS

The discrepancies $\mathfrak{D}^\pm(s)$ were calculated for s in the ranges $22\leqslant s\leqslant 32.7=(M-1)^2$ and $(M+1)^2=59.6\leqslant s\leqslant 76$. The pion-nucleon phase shifts used are those described in paper IV.[10] The results obtained are shown in Figs. 3 and 4. We now discuss the analysis of these results in terms of the pion-pion interaction in the $T=1$ and $T=0$ states.

The discontinuity in $f_0{}^T(s)$ as we cross the circle, $\Delta f_0{}^T(s)$, arises from the discontinuities in the invariant amplitudes $A^\pm(s,t)$, $B^\pm(s,t)$. The discontinuities in the invariant amplitudes across the circle are $2i\,\mathrm{Im}A_{\pi\pi}{}^\pm(s,t)$, $2i\,\mathrm{Im}B_{\pi\pi}{}^\pm(s,t)$ where $\mathrm{Im}A_{\pi\pi}{}^\pm(s,t)$, $\mathrm{Im}B_{\pi\pi}{}^\pm(s,t)$ represent the absorptive parts of the

[10] I am grateful to P. Menotti who provided me with tables of values of $\mathrm{Re}f_0{}^T(s_3)$ and $\mathrm{Im}f_0{}^T(s_3)$.

TABLE I. Values of $|B(s')|^{-1}$ for real s'.

s'	0	10	20	25	32.7	59.6	65	70	80	100
$\lvert B(s')^{-1}\rvert$	0.023	0.030	0.045	0.061	∞	∞	0.076	0.051	0.032	0.019

invariant amplitudes in channel 2, $\pi+\pi\rightarrow N+\bar{N}$. These are given as follows in terms of the helicity amplitudes $f_{\pm}^{J}(t)$ for this process,[11] which represent states with total angular momentum J and where the subscript is $+$ or $-$ according as the nucleon and antinucleon have the same or opposite helicities.

$$\begin{aligned}\mathrm{Im}A_{\pi\pi}^{(\pm)}(s,t)&=\frac{8\pi}{p_-^2}\sum_{J=0}^{\infty}(J+\tfrac{1}{2})(ip_-q_3)^J\left[P_J(\cos\theta_3)\,\mathrm{Im}f_+^J(t)-\frac{M}{[J(J+1)]^{1/2}}\cos\theta_3 P_J'(\cos\theta_3)\,\mathrm{Im}f_-^J(t)\right],\\ \mathrm{Im}B_{\pi\pi}^{(\pm)}(s,t)&=8\pi\sum_{J=1}^{\infty}\frac{J+\frac{1}{2}}{[J(J+1)]^{1/2}}(ip_-q_3)^{J-1}P_J'(\cos\theta_3)\,\mathrm{Im}f_-^J(t).\end{aligned}\tag{9}$$

q_3, p_-, and $\cos\theta_3$ are defined by the relations

$$t=4(1+q_3^2)=4(M^2-p_-^2),$$
$$\cos\theta_3=(s-p_-^2+q_3^2)/2ip_-q_3.$$

The isotopic spin superscripts for the $f_{\pm}^{J}(t)$ have been suppressed. $\Delta f_0^T(s_3)$ can now be expressed in terms of the $\mathrm{Im}f_{\pm}^{J}(t)$ by using Eqs. (2) and (3). The contribution to the discrepancy is given by the third term on the right-hand side of Eq. (8) which we shall denote by $\mathfrak{D}_{\pi\pi}^{\pm}(s)$. Equations (2), (3), (8), and (9) enable us to write

$$\mathfrak{D}_{\pi\pi}^{\pm}(s)=\int_{-\phi\max}^{\phi\max}d\phi'\int_{4\mu^2}^{t\max}dt'\sum_i K_i^{\pm}(s,\phi',t')\times\mathrm{Im}f_i^{\pm}(t'),\tag{10}$$

where $f_i^{\pm}(t)$ are the relevant helicity amplitudes $f_{\pm}^{J}(t')$ which may contribute and $K_i^{\pm}(s,\phi',t')$ are appropriate kernels which will be complex. The ϕ' integration refers to the integration around the circle, a point s' on the circle being represented as $(M^2-1)e^{i\phi'}$. The limit of integration $\phi_{\max}$ is normally taken to be 66°. Above this angle it has been shown that the partial-wave expansion (9) breaks down and so we conveniently take this angle as the limit of our "front of the circle" region. We may perform the ϕ' integration in Eq. (10) and rewrite this as

$$\mathfrak{D}_{\pi\pi}^{\pm}(s)=\int_{4\mu^2}^{t\max}dt'\sum K_i^{\pm}(s,t')\,\mathrm{Im}f_i^{\pm}(t').\tag{11}$$

The kernels $K_i^{\pm}(s,t)$ can be evaluated using Eqs. (2), (3), (9), and (10). Equation (11) thus provides the link which enables us to obtain information about the helicity amplitudes $f_{\pm}^{J}(t)$ from the calculated values of $\mathfrak{D}_{\pi\pi}^{\pm}(s)$.

The analysis may be carried a stage further by relating the helicity amplitudes $f_{\pm}^{J}(t)$ to the phase shifts δ_J^T for pion-pion scattering. The relationship is due to unitarity which requires the phase of $f_{\pm}^{J}(t)$ for $4\mu^2\leqslant t\leqslant 16\mu^2$ to be $\delta_J(t)$. This enables us to write approximate integral equations for $f_{\pm}^{J}(t)$.

The helicity amplitudes are analytic in the t plane with the exception of cuts from $-\infty$ to $a=4\mu^2(1-\mu^2/4M^2)$ and from $4\mu^2$ to $+\infty$. $\mathrm{Im}f_{\pm}^{J}(t)$ is determined for $0\leqslant t\leqslant a$ by the Born term alone. For $t<0$ it is related to pion-nucleon scattering and may be determined by an analytic continuation of pion-nucleon data. This continuation is performed in the usual way by making a partial-wave expansion: However, for $t<-25\mu^2$ this partial-wave expansion ceases to converge so that we cannot determine $\mathrm{Im}f_{\pm}^{J}(t)$ beyond this point.

We may use the analyticity properties of $f_{\pm}^{J}(t)$ to write the following approximate equation[12,13]:

$$f_{\pm}^{J}(t)\exp[-u_J(t)]=\frac{1}{\pi}\int_{-\infty}^{a}dt'\frac{\exp[-u_J(t')]\,\mathrm{Im}f_{\pm}^{J}(t')}{t'-t},\tag{12}$$

where

$$u_J(t)=\frac{t}{\pi}\int_{4\mu^2}^{\infty}dt'\frac{\delta_J(t')}{t'(t'-t)}.$$

The approximation made in (12) is to neglect other than two-pion intermediate states on the cut $t>16\mu^2$. We might expect this to be a good approximation for values of t somewhat larger than $16\mu^2$ where the cross section for four-pion processes should still be small. For energies appreciably above $16\mu^2$ many-pion proc-

TABLE II. Values of $|B(s')|^{-1}$ for $s'=(M^2-1)e^{i\phi'}$.

ϕ'	0	15°	30°	60°	90°
$\lvert B(s')\rvert^{-1}$	0.075	0.057	0.038	0.022	0.016

[11] M. Jacob and G. C. Wick, Ann. Phys. (N. Y.) 7, 404 (1959).

[12] R. Omnes, Nuovo Cimento 8, 316 (1958).

[13] W. Frazer and J. R. Fulco, Phys. Rev. 117, 1603 (1960).

esses will play a significant role. To minimize the effect of these we use a subtracted form of Eq. (12). Since we cannot calculate $\mathrm{Im}f_{\pm}^{J}(t)$ for $t<-25\mu^2$, we have to cut off the integral in Eq. (12) at this energy. To justify this neglect of the cut $t<-25\mu^2$ we again need subtractions in Eq. (12). The point $t=0$ is conveniently chosen as a subtraction point since the subtraction constants at this point are related to the pion-nucleon forward scattering amplitudes.[14,15]

So we might expect Eq. (12), suitably subtracted, to determine the helicity amplitudes $f_{\pm}^{J}(t)$ for $4\mu^2\leqslant t\leqslant 16\mu^2$, or perhaps to slightly higher values of t, in terms of the pion-pion phase shift $\delta_J(t)$. The helicity amplitudes in turn are related to the quantities $\mathfrak{D}_{\pi\pi}{}^{\pm}(s)$ by Eq. (11). Thus these two equations relate the quantities $\mathfrak{D}_{\pi\pi}{}^{\pm}(s)$, which we have calculated from low-energy pion-nucleon scattering data, to the pion-pion phase shifts $\delta_J(t)$. We may now proceed to discuss the analysis of our calculated values of $\mathfrak{D}^{\pm}(s)$ in terms of pion-pion phase shifts.

A. Analysis of $\mathfrak{D}^{-}(s)$

$\mathfrak{D}^{-}(s)$ corresponds to isotopic spin $T=1$ in channel 2. A pair of pions having $T=1$ must have a total angular momentum J which is odd.

Experiments on the production of pions in pion-nucleon interactions and on proton antiproton annihilation into pions have shown that a pion-pion "resonance" known as the ρ meson, with an energy of about 750 MeV and having $T=J=1$, appears to be the dominant feature in the $T=1$ two-pion system at reasonably low energies.[6] The nucleon form factor data seem to be well described by a model which approximates to the $T=1$ two-pion states by the ρ meson alone. Consequently we shall examine whether the data for $\mathfrak{D}^{-}(s)$ can be explained in terms of the exchange of a ρ meson without taking further account of the two-pion exchange term. Before doing this we discuss briefly the analysis of the nucleon form factor[16] data in terms of the ρ meson.

The Nucleon Form Factors

The electric and magnetic nucleon isovector form factors $F_1{}^{v}(t)$, $F_2{}^{v}(t)$ obey the dispersion relations

$$F_1{}^{v}(t)=\frac{e}{2}+\frac{t}{\pi}\int_4^{\infty}\frac{\mathrm{Im}F_1{}^{v}(t')dt'}{t'(t'-t)},$$
$$F_2{}^{v}(t)=\frac{eg}{2M}+\frac{t}{\pi}\int_4^{\infty}\frac{\mathrm{Im}F_2{}^{v}(t')dt'}{t'(t'-t)}, \tag{13}$$

where g is the (anomalous) gyromagnetic ratio. Unitarity relates $\mathrm{Im}F_{1,2}{}^{v}(t)$ to the $T=1$ pion-pion phase shift and to certain linear combinations of the helicity amplitudes and in particular tells us that these spectral functions are zero when the pion-pion phase shift $\delta_1(t)$ is zero. If we are taking account of the ρ meson alone, since this is reasonably narrow and also since we only compare Eq. (13) with experimental results for $t\leqslant 0$, it is a good approximation to replace $\mathrm{Im}F_{1,2}{}^{v}(t)$ by δ functions,

$$\mathrm{Im}F_i{}^{v}(t)=\alpha_i\delta(t-t_R), \tag{14}$$

where $t_R\approx 28$ for the ρ meson. The linear combinations of the helicity amplitudes which are related to $\mathrm{Im}F_i{}^{v}(t)$ by unitarity are

$$\Gamma_1(t)=M/(M^2-t/4)[(t/4\sqrt{2}M)f_-{}^{1}(t)-f_+{}^{1}(t)],$$
$$\Gamma_2(t)=\tfrac{1}{2}(M^2-t/4)^{-1}[f_+{}^{1}(t)-(M/\sqrt{2})f_-{}^{1}(t)]. \tag{15}$$

If we again make a δ-function approximation[17]

$$\mathrm{Im}\Gamma_i(t)=\pi C_i\delta(t-t_R), \tag{16}$$

then unitarity relates α_i, C_i and the pion-pion phase shift. Representing this phase shift by a resonance formula

$$e^{i\delta_1}\sin\delta_1=\gamma q_3{}^{3}/(t_R-t-i\gamma q_3{}^{3}),$$

where q_3 is the pion momentum in the center-of-mass system, the relation is

$$\alpha_i=-\pi eC_i t_R{}^{1/2}/\gamma. \tag{17}$$

Substituting from Eq. (14) in Eqs. (13) gives

$$F_1{}^{v}(t)=(e/2)[1+a/(t_R-t)],$$
$$F_2{}^{v}(t)=(eg/2M)[1+b/(t_R-t)]. \tag{18}$$

Here, $a=-2C_1/(\gamma t_R{}^{1/2})$, $b=-(2M/g)C_2/(\gamma t_R{}^{1/2})$. Equations (18) give agreement with the experimental data for $a\approx b\approx 1.6$. This gives the results

$$C_2\approx(g/M)C_1\approx 0.27C_1, \tag{19a}$$
$$\gamma=-2C_1/(1.6t_R{}^{1/2}). \tag{19b}$$

δ-Function Fit to $\mathfrak{D}^{-}(s)$

We shall now attempt to fit the data for $\mathfrak{D}^{-}(s)$ shown in Fig. 3 with a δ-function approximation to the helicity amplitudes $f_+{}^{1}(t)$, $f_-{}^{1}(t)$, to correspond to the ρ meson. We write

$$\mathrm{Im}f_{\pm}{}^{1}(t)=C_{\pm}\delta(t-t_R). \tag{20}$$

Equations (15) and (16) may be used to replace $C_{\pm}$ by C_1 and C_2:

$$C_+=-(\pi/2)(C_2t_R+2MC_1),$$
$$C_-=-\pi\sqrt{2}(C_1+2MC_2). \tag{21}$$

We use Eq. (19a) so that there only remains one free parameter which we take to be C_1. The contribution

[14] J. S. Ball and D. Y. Wong, Phys. Rev. Letters **6**, 29 (1961).
[15] P. Menotti, Nuovo Cimento **23**, 931 (1961).
[16] See the article by W. R. Frazer, in *Dispersion Relations*, edited by G. R. Screaton (Oliver and Boyd, Edinburgh, 1961).
[17] J. Bowcock, N. Cottingham, and D. Lurié, Nuovo Cimento **19**, 142 (1961).

to the discrepancy $\mathfrak{D}_{\pi\pi}^{-}(s)$ may now be calculated and depends only on C_1.

Very good agreement with the calculated data for $\mathfrak{D}^{-}(s)$ is obtained with a value $C_1=-1.4$, taking $t_R=28$. This provides the entire energy dependence of $\mathfrak{D}^{-}(s)$: The remaining short-range terms are only required to contribute a small and constant amount. The integration on the circle was over the range $|\phi|\leqslant 60°$. The result is shown by the solid line in Fig. 3; the broken line represents the constant short-range term.

Unfortunately, the value obtained for C_1 is rather sensitive to the cutoff angle on the circle. For example, integrating to 90° instead of 60° gives a comparably good fit with the data and leads to a value of $C_1=-0.9$. This corresponds to the results obtained in paper IV where a good fit was obtained for $C_1=-1.33$ but this could be altered to -1.05 by allowing a somewhat energy-dependent short-range term. Such an energy-dependent term could probably have been provided by the part of the circle $60°\leqslant|\phi|\leqslant 90°$. We conclude that $|C_1|$ is probably less than 1.4 and that

$$-1.4\leqslant C_1\leqslant -0.9.$$

The form of $\mathfrak{D}^{-}(s)$ does not depend very critically on the value of t_R. An optimum fit is obtained for t_R in the neighborhood of 28 but good agreement could still be obtained, for example, with two δ functions, the most important one at $t_R=28$ but a second one at, say, $t_R=16$ to correspond to the ζ meson.[18] This would lead to a smaller $|C_1|$ for the $t_R=28$ term.

An attempt to relate the helicity amplitudes $f_{\pm}'(t)$ to the pion-pion phase shift $\delta_1(t)$ for a resonance at $t\approx 28$ using the integral Eq. (12) so far has not been successful. This is presumably due to the necessity of taking account of inelastic processes. A discussion of this problem is given in paper IV.

It is still possible to obtain information about the $T=1$ pion-pion phase shift, without solving an integral equation. This is through Eq. (19b) which relates C_1 to the width of the pion-pion resonance. Thus a value of $C_1=-1.4$ gives $\gamma=0.33$ and the half-width of the resonance at half maximum 60 MeV. $C_1=-0.9$ gives $\gamma=0.21$ and the half-width 40 MeV. So the limits which we placed on C_1 would suggest that the half-width of the resonance should be between 60 and 40 MeV. This is in good agreement with experimental results for the width of the ρ meson.[18]

It should be pointed out that the derivation of Eq. (19b) involved a neglect of inelastic processes. This could be a source of inaccuracy.

B. Analysis of $\mathfrak{D}^{+}(s)$

$\mathfrak{D}^{+}(s)$ corresponds to isotopic spin $T=0$ in channel 2. A pair of pions having $T=0$ must have even angular momentum J. Since we are chiefly concerned with reasonably low energies in channel 2 we might expect that only the s wave should be important, so we attempt to fit the data for $\mathfrak{D}^{+}(s)$ in terms of the s-wave term only.

There is only one s-wave helicity amplitude, $f_{+}^{0}(t)$. Equation (11) then becomes

$$\mathfrak{D}_{\pi\pi}^{+}(s)=\int_{4\mu^2}^{t\max} dt'\, K_{+}^{0}(s,t')\,\mathrm{Im}f_{+}^{0}(t'), \qquad (22)$$

and $f_{+}^{0}(t')$ is related to $\delta_0(t')$ by a suitably subtracted form of Eq. (12). It appears that two subtractions are needed in this case. The argument for this is as follows. For $a\gtrsim t\gtrsim -25\mu^2$ where the partial-wave expansion is valid, $\mathrm{Im}f_{+}^{0}(t)$ is found to be well approximated in terms of the $T=\frac{3}{2}$, $J=\frac{3}{2}$ pion-nucleon resonance alone. This contributes to $\mathrm{Im}f_{+}^{0}(t)$ a term which behaves like t as $t\to-\infty$ [see Eq. (9)]. Consequently, it would seem that two subtractions should be made in Eq. (12) to bring the integral into a convergent form and thus reduce the sensitivity to the cutoff position. A further discussion on this is given in paper IV.

We use the values for the two subtraction constants obtained by Menotti[15] and evaluate the integral equation (12) using the same pion-nucleon data as in IV. To analyze the data for $\mathfrak{D}^{+}(s)$ we start with various forms of the $T=0$ phase shift which we express in a two-parameter form, on the basis of a one-pole approximation to the N function in the N/D solution to the Chew-Mandelstam equations. The two parameters are the position and residue of this pole. These values are varied over a wide range and for each pair of values the integral equation (12) is solved. The results are substituted in Eq. (22) and compared with the experimental data for $\mathfrak{D}^{+}(s)$ shown in Fig. 4. Before discussing the results we briefly summarize the phase-shift parametrization procedure.

One-Pole Pion-Pion Solutions[19]

The $T=0$, $J=0$ pion-pion amplitude in invariant form is

$$A(\nu)\equiv[(\nu+1)/\nu]^{1/2}e^{i\delta_0}\sin\delta_0. \qquad (23)$$

δ_0 is real in the elastic region and ν is $t/4-1$. $A(\nu)$ has cuts on the real axis for $-\infty<\nu\leqslant -1$, $0\leqslant\nu<\infty$.

We write

$$A(\nu)=N(\nu)/D(\nu),$$

where $N(\nu)$ has only a cut for $-\infty<\nu\leqslant -1$ and $D(\nu)$ for $0\leqslant\nu<\infty$. On $0\leqslant\nu<\infty$, $\mathrm{Im}D(\nu)$ is given by

$$\mathrm{Im}D(\nu)=-N(\nu)R[\nu/(\nu+1)]^{1/2},$$

where R is the ratio of the total to the elastic cross section for the $T=0$ π-π interaction. $N(\nu)$ is real on $0\leqslant\nu<\infty$. Putting $R=1$ we may write the dispersion

[18] See D. L. Stonehill and H. L. Kraybill (to be published).

[19] See W. R. Frazer, reference 16 for a detailed discussion.

relation for $D(\nu)$

$$D(\nu)=1-\frac{\nu-\nu_0}{\pi}\int_0^\infty d\nu'\left(\frac{\nu'}{\nu'+1}\right)^{1/2}\frac{N(\nu')}{(\nu'-\nu_0)(\nu'-\nu)}. \quad (24)$$

We have made one subtraction at ν_0 and put $D(\nu_0)=1$. We now approximate to $N(\nu)$ by a single pole at $\nu=\nu_1$, $\nu_1<0$, with residue Γ.

$$N(\nu)=\Gamma/(\nu-\nu_1). \quad (25)$$

Substituting this in Eq. (24) and taking $\nu_0=\nu_1$ gives

$$D(\nu)=1-\frac{\Gamma}{\pi}(\nu-\nu_1)\int_0^\infty d\nu'\left(\frac{\nu'}{\nu'+1}\right)^{1/2}\times\frac{1}{(\nu'-\nu_1)^2(\nu'-\nu)}. \quad (26)$$

Since $D(\nu_1)=1$, Eq. (25) is equivalent to

$$\mathrm{Im}A(\nu)=-\pi\Gamma\delta(\nu-\nu_1),$$

for $\nu\leqslant-1$, so our procedure is effectively to replace the left-hand cut in $A(\nu)$ by a δ function.

So, corresponding to every pair of values of the parameters Γ, ν_1, we obtain a solution for the $T=0$ pion-pion phase shift $\delta_0(\nu)$, which is determined by Eqs. (23), (25), and (26).

Comparison with Data for $\mathfrak{D}^+(s)$

When $\mathfrak{D}_{\pi\pi}{}^+(s)$ is calculated for different values of ν_1, Γ, for s lying in the ranges $20\leqslant s\leqslant 32.2$, $59.6\leqslant s\leqslant 76$, the result is found not to be very sensitive to the values of the two parameters simultaneously. For example we may say that $\mathfrak{D}_{\pi\pi}{}^+(s)$ is rather insensitive to the value of ν_1 (for $\nu_1\leqslant-5$), but for any value of ν_1, the requirement that $\mathfrak{D}_{\pi\pi}{}^+(s)$ should provide the energy dependence shown by the experimental results determines the value of Γ. So we obtain a one-parameter family of phase shifts which give agreement with the data for $\mathfrak{D}^+(s)$. Typical values of ν_1 and Γ with the corresponding scattering lengths are shown in Table III.

The corresponding phase shifts are plotted in Fig. 5. The values of $\mathfrak{D}_{\pi\pi}{}^+(s)$ for these solutions are shown in Fig. 4 where they are compared with the $\mathfrak{D}^+(s)$ data. The short-range contributions to $\mathfrak{D}^+(s)$ have been replaced by constants lying in the range $-0.0051\leqslant C\leqslant-0.0048$. Compared with the magnitudes of $\mathfrak{D}_{\pi\pi}{}^+(s)$ these constant terms are quite small. We cannot appreciably improve the fit in Fig. 4 by giving the short-range terms a simple energy dependence.

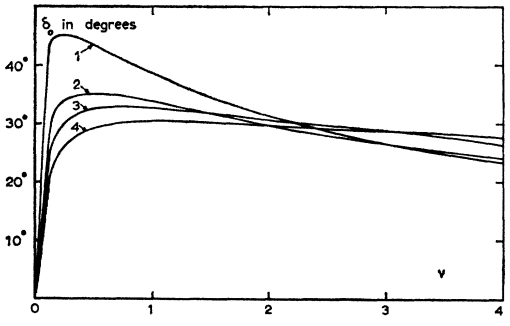

FIG. 5. $\delta_0(\nu)$. The phase-shift solutions 1 to 4 of Table III.

We are not particularly concerned by the poor agreement with the value of $\mathfrak{D}^+(s)$ at $s=22$. The errors involved in the calculation of $\mathfrak{D}^+(s)$ are largest for the values of s nearest to the origin, where high partial waves are contributing and so we are least concerned with the fit to the data at these energies. It is probable that an over-all improvement to the fit could be obtained by taking account of d waves; in our opinion, however, a quite satisfactory agreement within the errors involved is obtained by taking account only of s waves in the pion-pion amplitude.

The fact that different forms for the pion-pion phase shift lead to similar values of $\mathfrak{D}_{\pi\pi}{}^+(s)$ is understood from Eq. (22). This equation involves an integral over the imaginary part of the helicity amplitude $\mathrm{Im}f_+{}^0(t')$ with a weighting function $K_+{}^0(s,t')$. A more pronounced low-energy behavior of $\mathrm{Im}f_+{}^0(t')$ can thus be compensated for by a more rapid falloff with increasing t'. This is understood from the phase-shift solutions in Table III. The solutions with large scattering lengths correspond to the pole positions ν_1 closest to the physical region. The nearer the pole is to the physical region the more rapidly will the phase shift falloff at high energies. This behavior is reflected in that of $\mathrm{Im}f_+{}^0(t')$.

TABLE III. $T=0$ pion-pion phase-shift parameters in the "one-pole" approximation.

Solution	Pole position ν_1	Residue Γ	Scattering length a_0
1	−5	5	4.13
2	−10	7	2.02
3	−30	16	1.58
4	−100	42	1.29

In paper IV an alternative parametrization of the $T=0$ phase shift is also used. This is based on a conformal mapping of the ν plane, cut from -1 to $-\infty$, into the unit circle and $N(\nu)$ is approximated by two terms of a polynomial in the transformed variable. This permits solutions in which the phase shift changes sign. One solution in particular in which the phase shift was negative at first, with a negative scattering length, and then became positive was found to give good agreement with the calculated discrepancies. We attempted to fit our data with this phase shift but found that it badly failed to give agreement with the energy dependence of our results for $\mathfrak{D}^+(s)$ and so we reject this solution for the phase shift.

In the next section we use other experimental data, from the process $p+d\rightarrow \mathrm{He}^3+2\pi$, to distinguish between the different phase shifts which are in agreement with our data for $\mathfrak{D}^+(s)$.

4. THE PROCESS $p+d\rightarrow \mathrm{He}^3+2\pi$

This process has been investigated by Abashian, Booth, and Crowe.[7,20,21] They measured the recoil spectrum of the He^3 ions produced at a fixed angle in the laboratory system, the energy of the proton beam being kept fixed. Their results are shown in Fig. 6 where the number of counts is plotted against the He^3 momentum.

The broken curve in Fig. 6 represents the relativistic phase space adjusted for the experimental resolution and normalized to fit the low-momentum points. It is seen that there is a pronounced peak above the phase-space curve in the momentum region which corresponds to energies just above threshold in the two-pion system. It was surmized that this could be due to an interaction

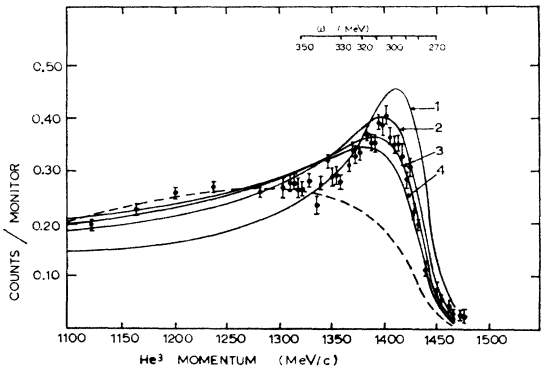

FIG. 6. Comparison with experimental data for $p+d\rightarrow \mathrm{He}^3+2\pi$ with solutions 1 to 4 of Table III. The dashed curve represents the relativistic phase-space factor.

between the two pions at energies close to threshold. When the analogous experiment $p+d\rightarrow \mathrm{H}^3+2\pi$ was performed, no such peak was observed. Consequently, if the peak is to be explained by an interaction between the pions, this interaction must take place in the $T=0$ state.

An analysis of the data was made, introducing a final-state interaction between the two $T=0$ pions.[21] The final-state interaction was expressed in terms of an enhancement factor modifying the phase-space distribution. According to Watson[22] this enhancement factor should be $|A(\nu)|^2$, where $A(\nu)$ is the $T=0$ pion-pion amplitude, given by Eq. (23). With this procedure it was shown that good agreement with the experimental data could be obtained using a $T=0$

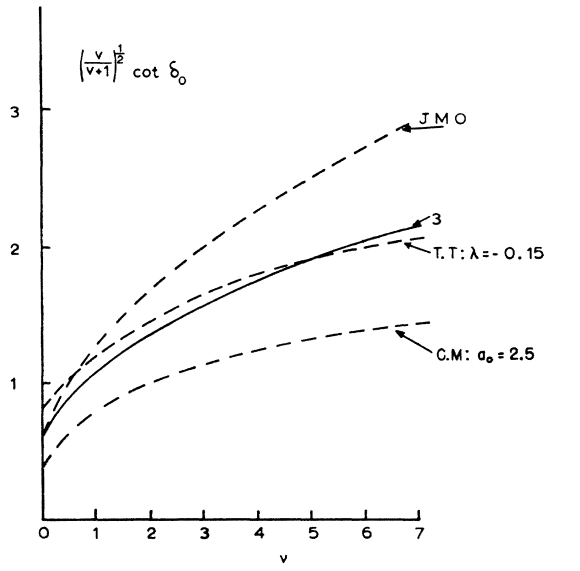

FIG. 7. $[\nu/(\nu+1)]^{1/2}\cot\delta_0$ for solution 3, solid line; also solution of Jacob *et al.*, denoted by JMO; of Taylor and Truong, denoted by T.T.; $\lambda=-0.15$; and the Chew-Mandelstam effective-range solution, denoted by C.M., $a_0=2.5$.

phase shift with a scattering length $a_0\approx 2.5$. This phase shift satisfied the effective range formula of Chew and Mandelstam[23]: In the notation of Sec. 3 above it was a solution of our one-pole equations in which the pole position was effectively moved to $-\infty$ so that the function $N(\nu)$ was approximated by a constant. This phase shift, denoted by C.M., is shown in Fig. 7.

Some uneasiness was felt at the large value of the scattering length which was apparently needed: This seemed to lead to difficulties in an analysis of pion production in low-energy pion-nucleon interactions or of τ decay. The method of treating final-state interactions was re-analyzed by Jacob, Mahoux, and Omnes.[24] They pointed out that the amplitude $T(\nu)$ for the process $p+d\rightarrow \mathrm{He}^3+2\pi$ has a cut for real $\nu>0$, where $\nu=\frac{1}{4}t-1$, and t is the square of the total center-of-mass energy of the two pions. If final-state interactions involving the He^3 ions are neglected, then unitarity tells us that the phase of $T(\nu)$ for $0\leqslant\nu\leqslant 3$ is $\delta_0(\nu)$. The remaining singularities of $T(\nu)$ are unknown, the simplest approximation is to suppose that in the region of interest, which is the low-energy part of the two-pion cut (ν real and $0\leqslant\nu<3$), these should give a constant effect. $T(\nu)$ then takes the form:

$$T(\nu)=C\exp\left[\frac{\nu}{\pi}\int_0^\infty\frac{\delta_0(\nu')d\nu'}{\nu'(\nu'-\nu)}\right]. \tag{27}$$

This is the same result as Eq. (12) if we replace the integral over the left-hand cut by the constant C.

[20] A. Abashian, N. E. Booth, and K. M. Crowe, Phys. Rev. Letters **5**, 528 (1960).
[21] N. E. Booth, A. Abashian, and K. M. Crowe, Phys. Rev. Letters **7**, 35 (1961).
[22] K. M. Watson, Phys. Rev. **88**, 1163 (1952).
[23] G. F. Chew and S. Mandelstam, Phys. Rev. **119**, 467 (1960).
[24] M. Jacob, G. Mahoux, and R. Omnes, Nuovo Cimento **23**, 838 (1962).

Jacob *et al.*, claim to find agreement with the data, using $|T(\nu)|^2$ as an enhancement factor, for a phase shift obtained as a solution to the Chew-Mandelstam equations which had a scattering length $a=1.6$ and which is well approximated by a one-pole solution with $\nu_1\approx -5$. However, these authors did not take account of the experimental resolution in fitting the data: Because of this it is difficult to assess the quality of the agreement obtained with their phase-shift solution.

Jackson and Kane[25] have shown that if the phase shift satisfies the Chew-Mandelstam "effective range" formula, $T(\nu)$ and $A(\nu)$ are the same and so the two methods of treating final-state interactions are the same. This is clearly true since the right-hand side of Eq. (27) is the function $D^{-1}(\nu)$ (see Sec. 3) in an N/D solution for $A(\nu)$. If now we put $N(\nu)=$constant, to give an "effective range" solution for $\delta_0(\nu)$, then $A(\nu)\equiv N/D$ is the same as $T(\nu)$. When $\delta_0(\nu)$ differs appreciably from an effective range solution, the two enhancement factors will differ. This is clearly the case for the above solution of Jacob *et al.*, since we have seen that this is approximated by a one-pole solution with the pole at $\nu=-5$ which is close to the physical region.

It is not clear, however, that the enhancement factor $|T(\nu)|^2$ is preferable to $|A(\nu)|^2$. The derivation of Eq. (27) assumed that the contribution of the singularities other than from the two-pion interaction could be replaced by a constant. In this case $T(\nu)$ is the same as $A(\nu)$ if $A(\nu)$ has been derived in the same approximation of replacing the effect of the other singularities by a constant. In the derivation of $T(\nu)$ a better approximation would probably have been to replace the effect of these other singularities by a pole in just the same way as we have done for $A(\nu)$ in Sec. 3. If this pole is very far away from the physical region, it would be equivalent to a constant as used above. However, in the absence of information about the other singularities of $T(\nu)$, we must regard this pole position as arbitrary. We wish to point out that if this pole has the same position ν_1 as the pole used to represent the left-hand singularities in $A(\nu)$, where $A(\nu)$ is a one-pole solution as obtained in Sec. 3, then $T(\nu)$ and $A(\nu)$ are again the same. More generally, if the left-hand singularities of $A(\nu)$ are represented in a more complicated way, $T(\nu)$ and $A(\nu)$ are the same provided the remaining singularities in $T(\nu)$ are the same as those in $A(\nu)$ assuming both to have the same asymptotic behavior. This is easily seen to be true since both $A(\nu)$ and $T(\nu)$ have the same phase along the cut $0\leqslant\nu<\infty$ and their remaining singularities are the same.

In view of these arguments and for convenience of calculation we have used $|A(\nu)|^2$ as the enhancement factor to calculate the effects of our phase-shift solutions 1, 2, 3, 4 (Table III and Fig. 5). The results are shown in Fig. 6. Except for solution 1 the results have been normalized to the area under the experimental points. The experimental resolution shown in (20) has been taken into account. For 1, the calculated results have been somewhat scaled down in an attempt to improve the fit to the peak. It is clear that solution 1 gives too large an effect and solution 4 too small. The best agreement seems to be obtained with solution 3 $[(\nu_1=-30, a_0=1.58)$ (units $\hbar=\mu=c=1)]$ which gives good agreement over the whole momentum range.

A more systematic analysis might attempt to fit the results with the pole representing the remaining singularities of $T(\nu)$ in different positions. It seems probable, however, that the results will not be very sensitive to this pole position[25] and for solution 3 the difference between our result, where this pole is effectively at -30, and that of Jacob *et al.*, where it is at $-\infty$, is probably not great.

In Fig. 7 we plot $[\nu/(\nu+1)]^{1/2}\cot\delta_0$ both for our solution 3 and for Jacob's solution. These both have the same scattering length but because of the different pole positions they have different energy dependences. We also show in Fig. 7 $[\nu/(\nu+1)]^{1/2}\cot\delta_0$ for a phase shift obtained by Taylor and Truong[26] as a solution to the Chew-Mandelstam equations with $\lambda=-0.15$.

5. CONCLUSIONS

To simplify the task of isolating the two-pion exchange graphs from the other effects contributing to low-energy pion-nucleon scattering, new dispersion relations were derived for the s-wave amplitudes. These relations suppressed the contributions from unknown short-range processes and emphasized the low-energy features of interest. They were used to evaluate the two-pion exchange terms from low-energy pion-nucleon scattering data.

Figures 3 and 4 show the calculated values of the discrepancies $\mathfrak{D}^-(s)$ and $\mathfrak{D}^+(s)$, the superscripts $-$ and $+$ referring to isotopic spin $T=1$ and $T=0$ for the pion pair. These include unknown short-range contributions in addition to the two-pion terms but the dispersion relations were chosen so as to suppress these short-range effects and the results for $\mathfrak{D}^\pm(s)$ are well fitted with small constant terms due to short-range effects together with larger and strongly energy-dependent terms due to the two-pion exchange. It is quite clear from the characteristic energy dependences of the data in Figs. 3 and 4 that these are primarily due to the exchange of a pair of pions in the appropriate isotopic spin state, so that the relevant graphs have indeed been isolated from the experimental data.

The results for the two-pion exchange graphs were analyzed in terms of the pion-pion interaction in the $T=1$ and $T=0$ states, leading to the following conclusions:

[25] J. D. Jackson and G. L. Kane, Nuovo Cimento **23**, 444 (1962).

[26] J. G. Taylor and T. N. Truong (to be published).

A. The $T=1$ Pion-Pion Interaction

The data for $\mathfrak{D}^-(s)$ were very well fitted in terms of a single p-wave resonance at an energy of about 750 MeV, corresponding to the observed ρ meson. Combining the results of this analysis with electron-nucleon scattering data the half-width of this resonance at half maximum was calculated to lie between 40 and 60 MeV. To obtain these figures we neglected the effect of inelastic processes: It could be on account of the fairly high energy that these would lead to some modification in the result for the width.

There is no direct evidence for a contribution from the region of 550 MeV (ζ meson?). However, the calculated curve is not very sensitive to the two-pion energy and a smaller contribution at 550 MeV together with the ρ meson could still give good agreement.

B. The $T=0$ Pion-Pion Interaction

We defined $T=0$, pion-pion s-wave phase shifts in terms of two parameters, corresponding to the position and residue of the pole in one-pole approximate solutions to the Chew-Mandelstam equations. Fitting with the data for $\mathfrak{D}^+(s)$ only fixed one of these parameters, leaving us with a one parameter family of possible solutions. To distinguish between these, we used the experimental data for the process $p+d\rightarrow \mathrm{He}^3+2\pi$ and attempted to satisfy these in terms of a final-state $T=0$ pion-pion interaction. This enabled us to single out a phase shift which gave agreement both with these data and with the results for $\mathfrak{D}^+(s)$. This phase shift has a scattering length $a_0\approx 1.6$ and corresponds to a solution of the Chew-Mandelstam equations in which the left-hand cut is approximated by a δ function at $\nu=-30$. In Fig. 7, $[\nu/(\nu+1)]^{1/2}\cot\delta_0$ is plotted against ν for this phase shift δ_0. It is seen that it lies close to the solution to the Chew-Mandelstam equations obtained by Taylor and Truong[26] for a "coupling constant" $\lambda=-0.15$, although this has a smaller scattering length than our solution. Our phase shift gives the value $\lambda=-0.18$. [-5λ is $A(\nu)$ at $\nu=-\frac{2}{3}$.] The Chew-Mandelstam effective-range solution with $a_0=2.5$ is also shown in Fig. 7 for comparison.

ACKNOWLEDGMENTS

I am indebted to G. C. Oades for valuable discussions, for his help with the computer programming, and for permission to use some of his autocode programs. I should like to thank Professor J. Hamilton for his helpful advice and criticism, and Professor J. D. Jackson for valuable comments.

I am grateful to W. Klein and K. Kölbig for their help with some of the numerical computations.

I should also like to thank Professor L. Van Hove for his hospitality at the Theory Division of CERN where the earlier part of this work was carried out.